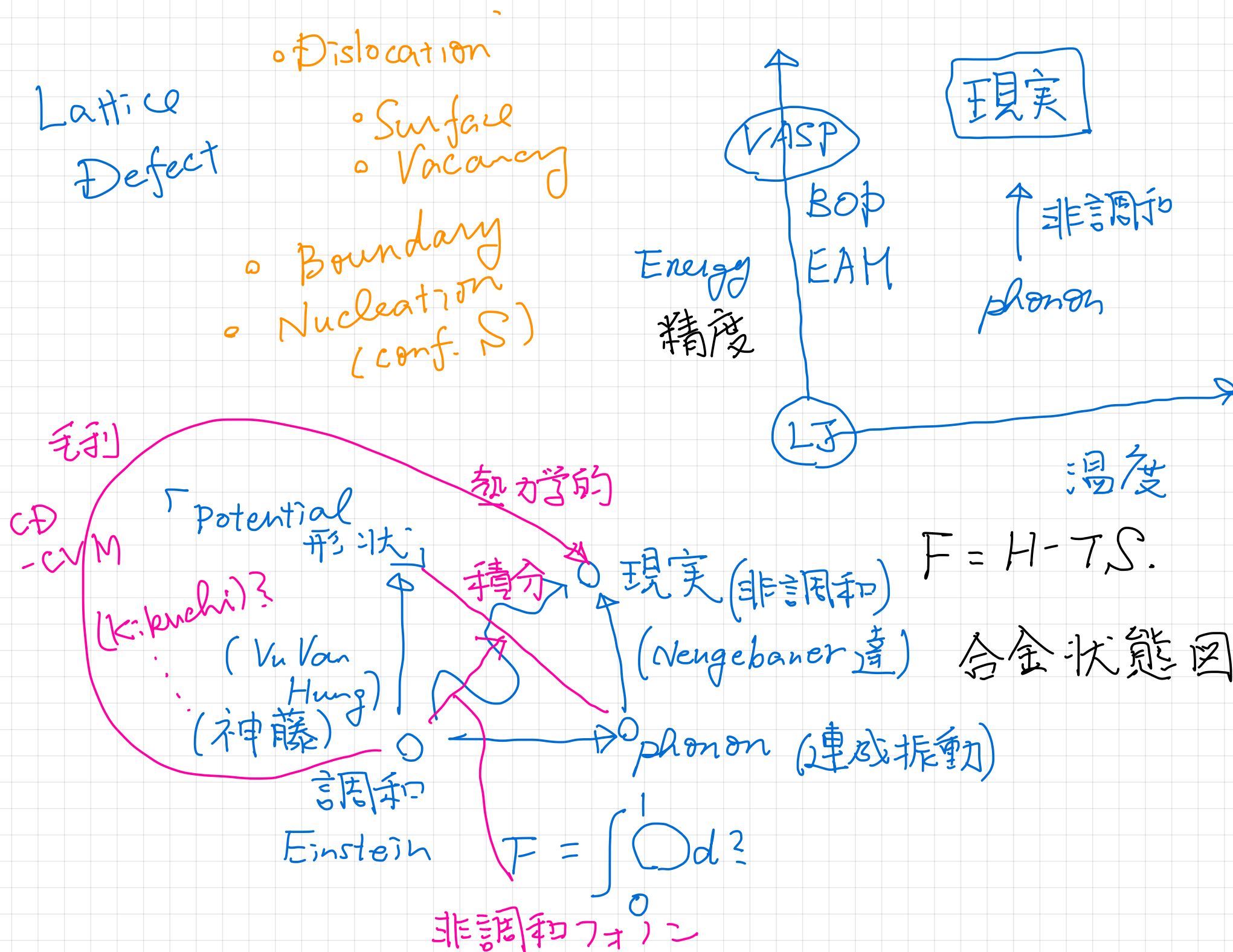


格子欠陥自由エネルギーの非調和性

合金状態図研究会 第4回

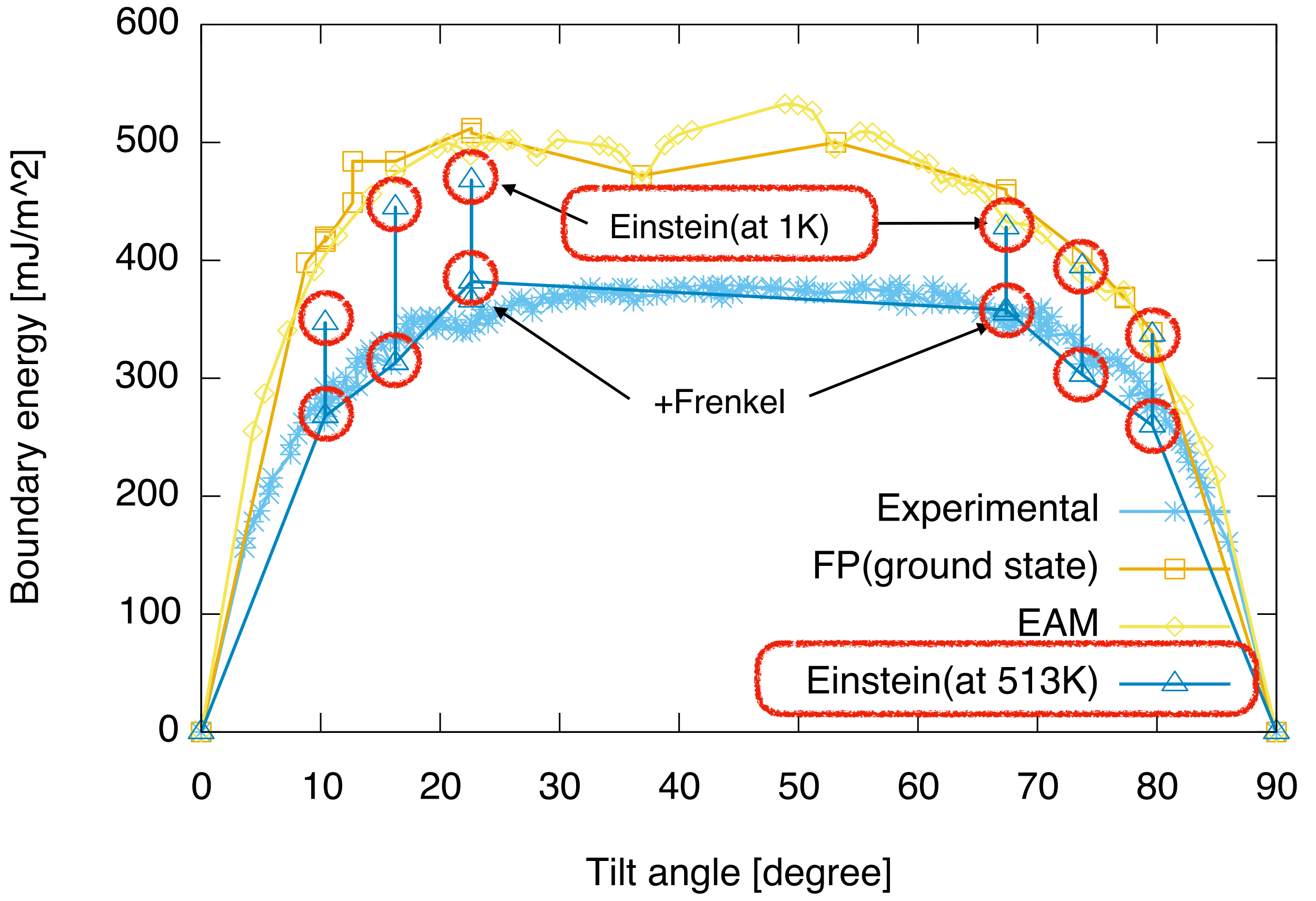
関西学院大・工 西谷滋人

2023/12/9 at 小倉

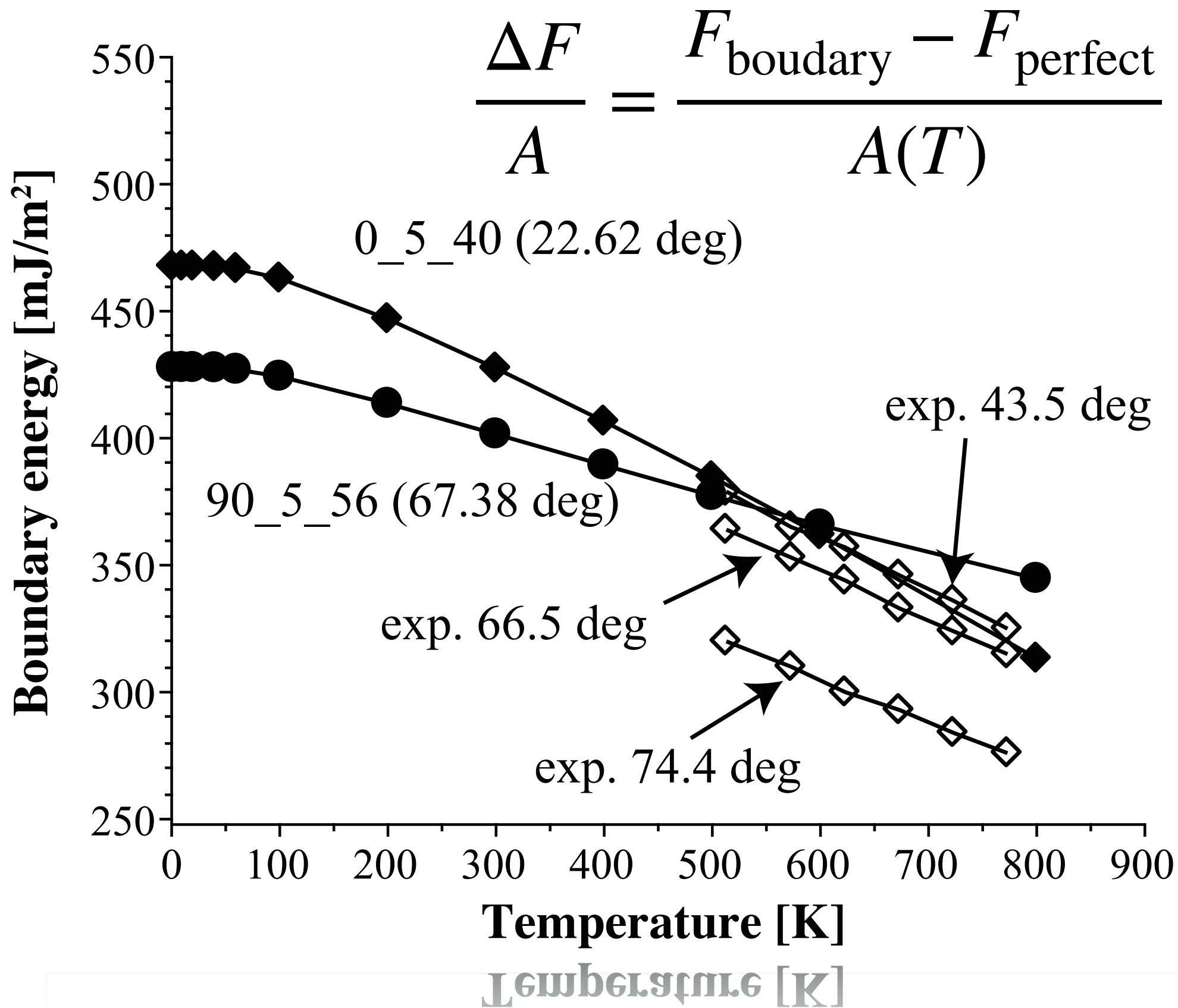


Tilt boundary
(Einstein)

Al <100> tilt boundary energy



temperature dependency of BE





ELSEVIER

Contents lists available at [ScienceDirect](https://www.sciencedirect.com)

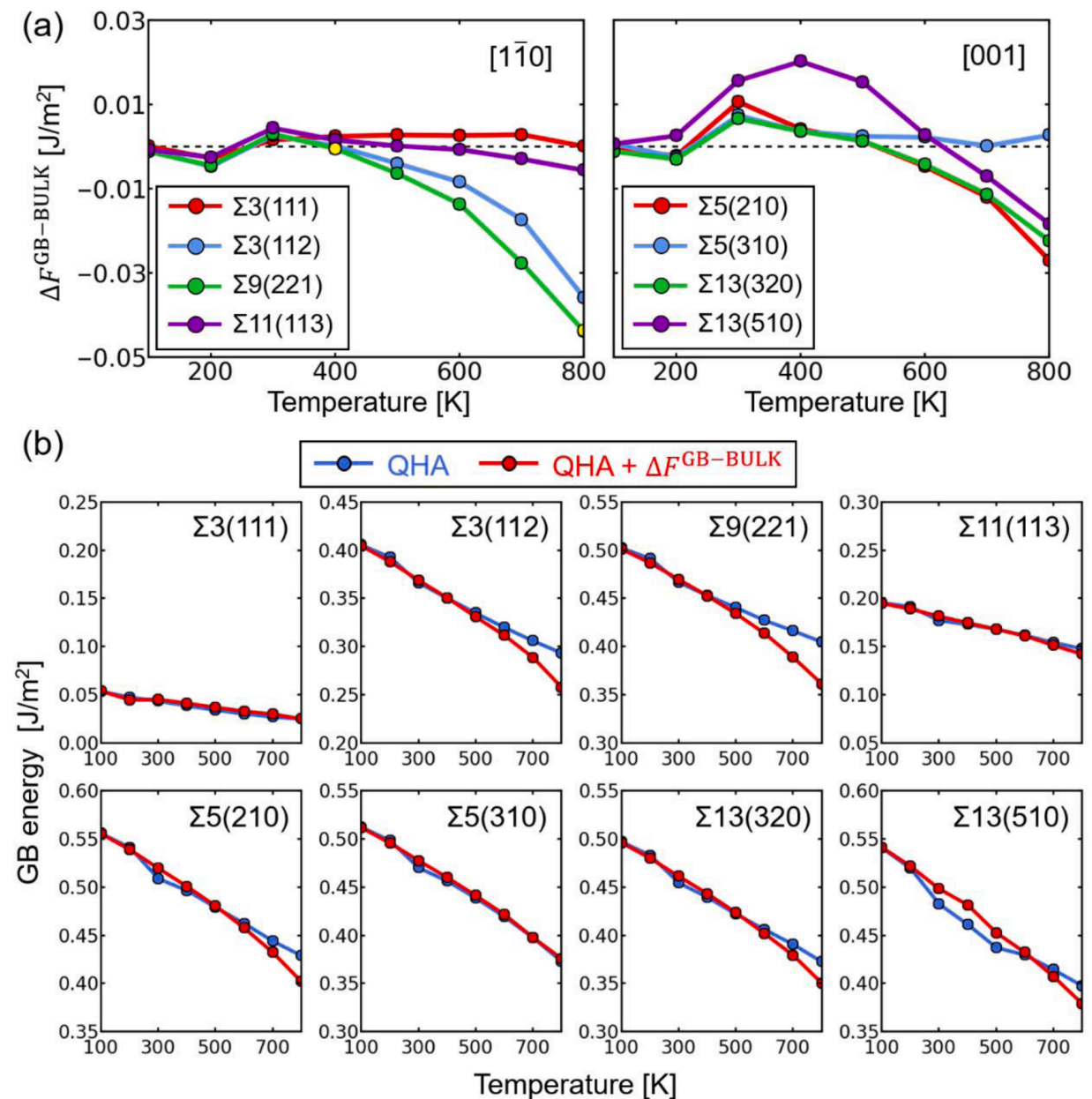
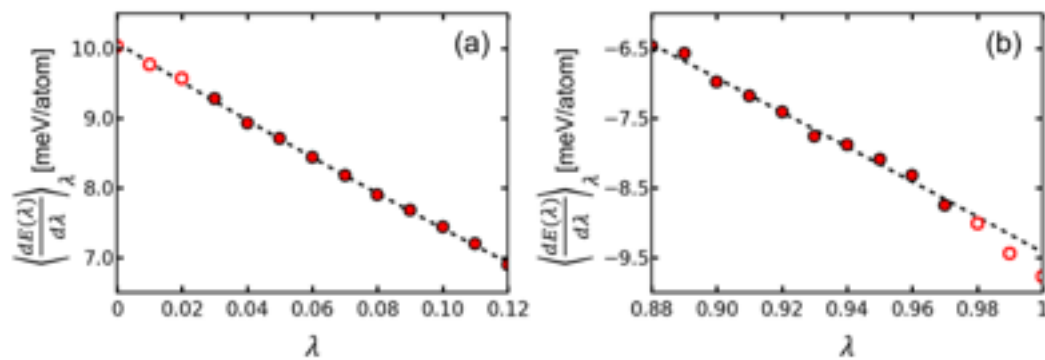
Scripta Materialia

journal homepage: www.journals.elsevier.com/scripta-materialia

Anharmonicity in grain boundary energy for Al: Thermodynamic integration with artificial-neural-network potential

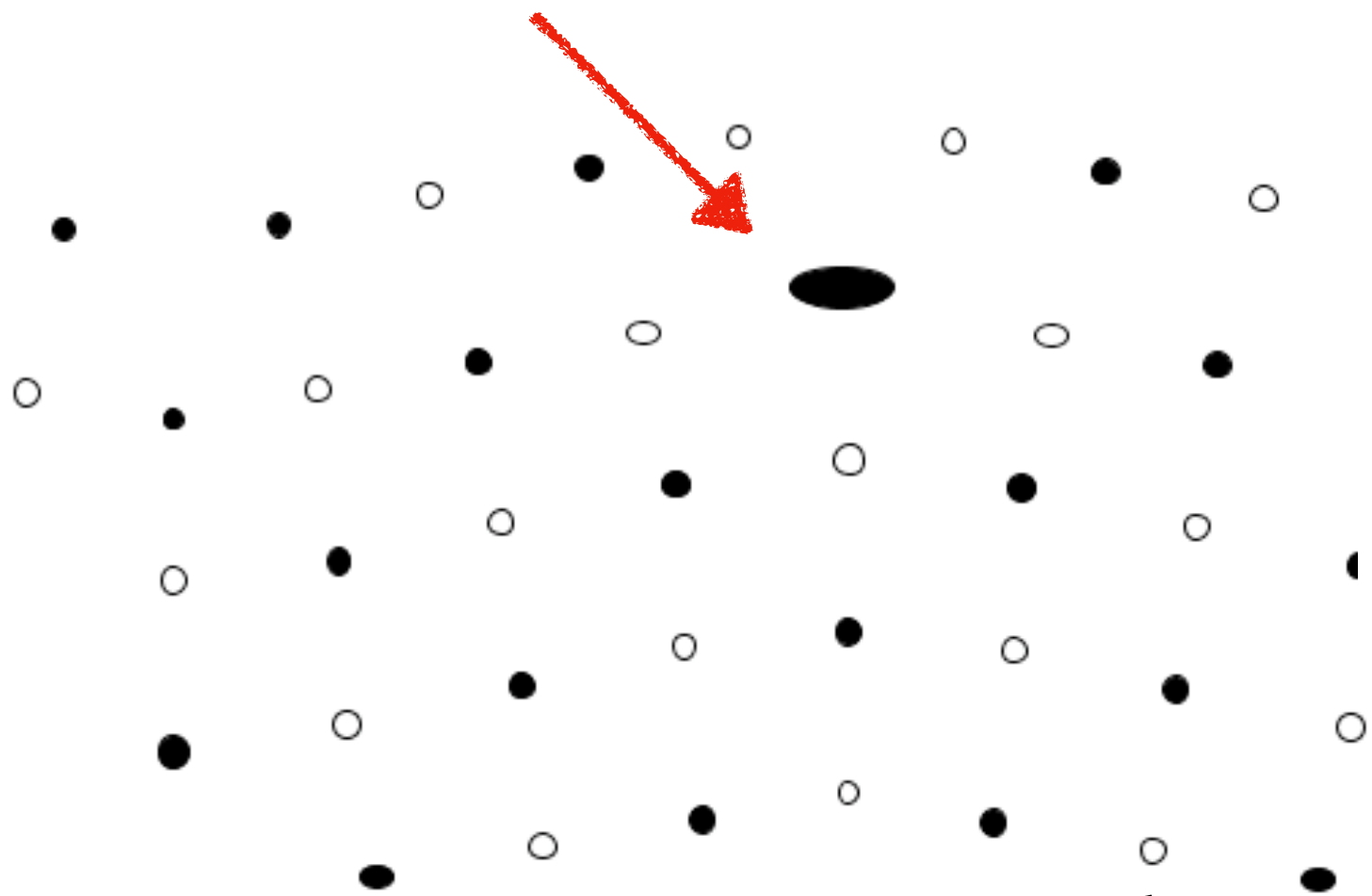
M. Matsuura^a, T. Yokoi^{a,*}, Y. Ogura^a, K. Matsunaga^{a,b}

Using ANN potential and Thermodynamical Integration from QHA, with Langevin thermostat



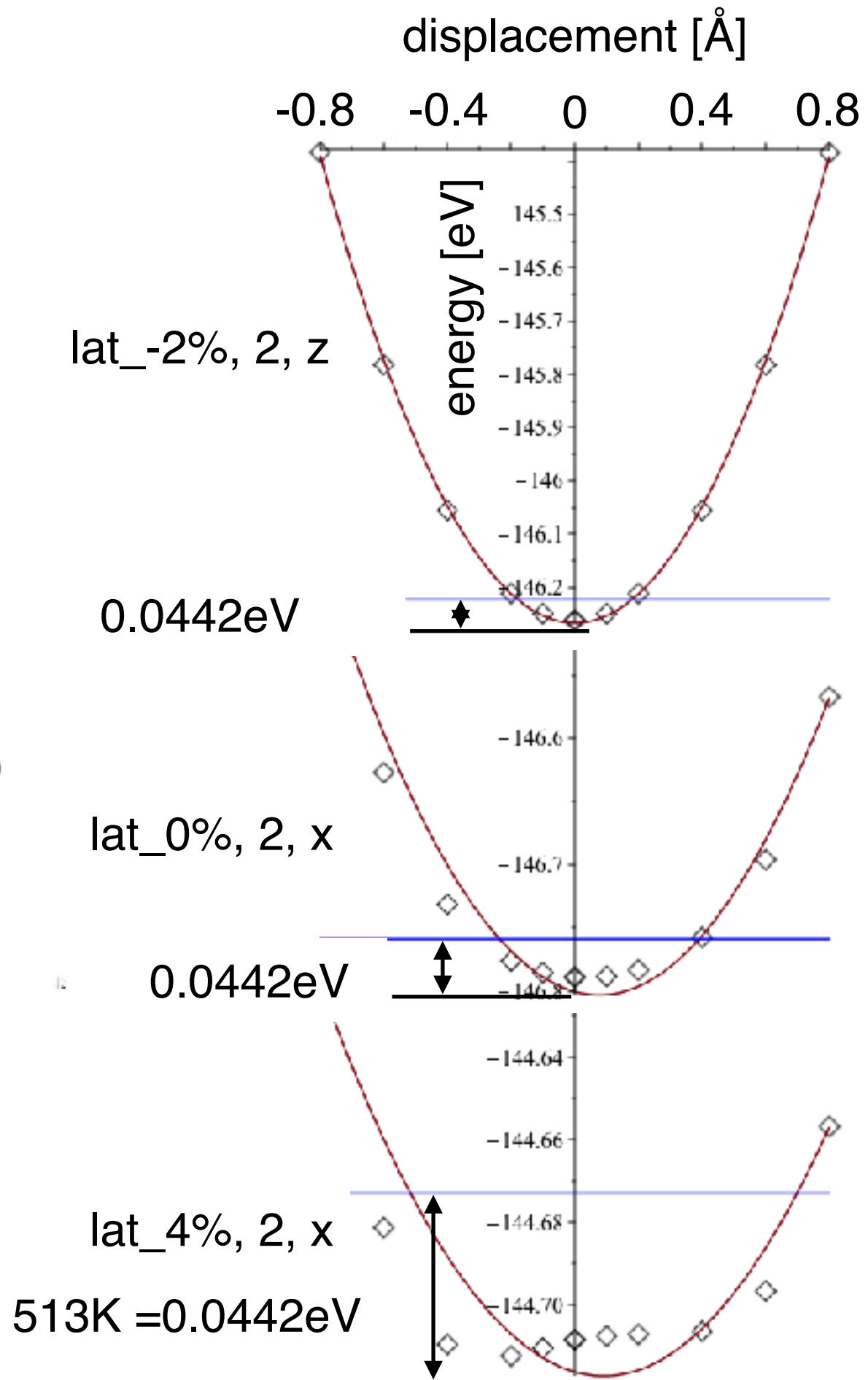
0_5_40 einstein

GN dislocation core



$$\Theta_{ij} = \frac{h\nu_{ij}}{k_B}$$

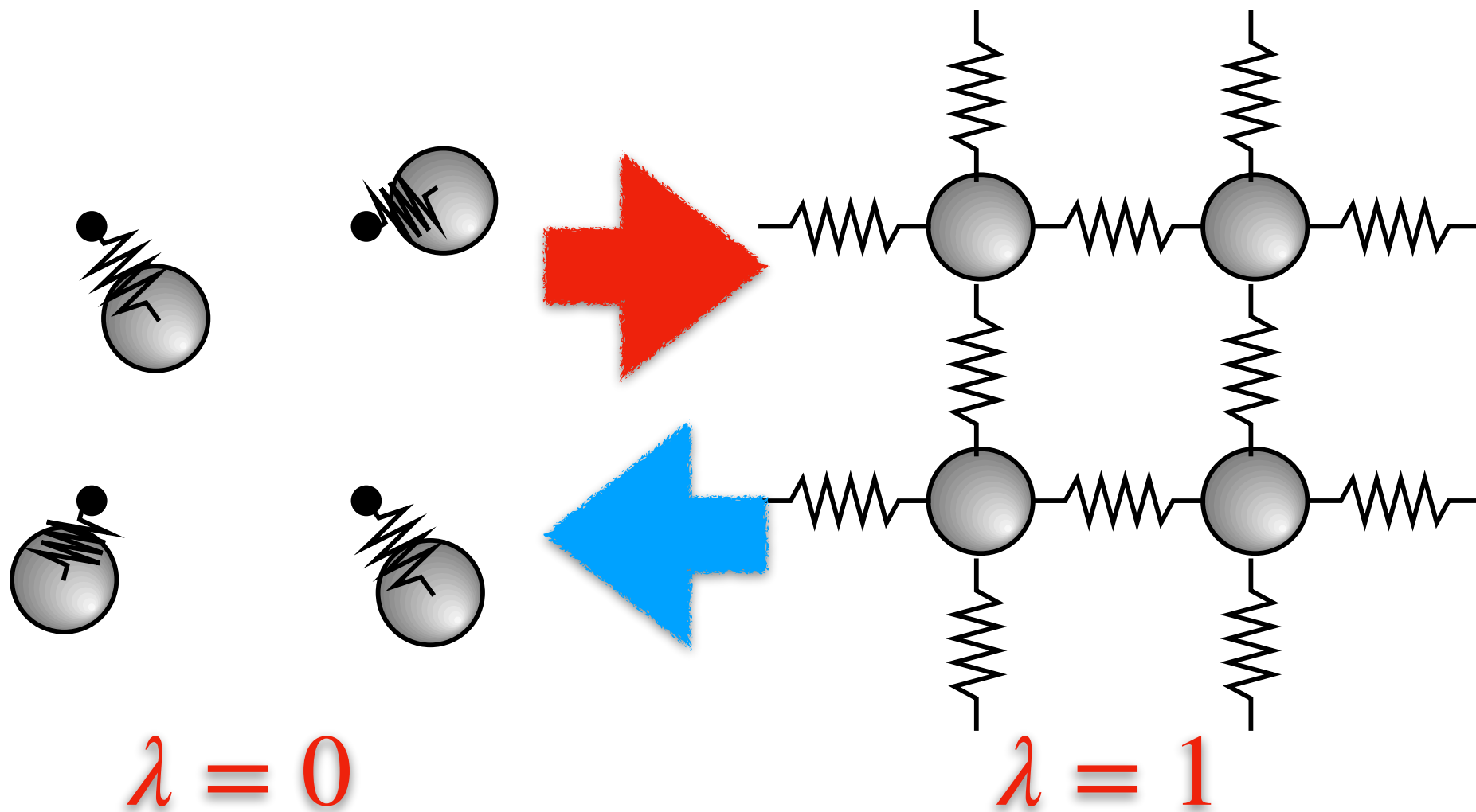
$$\nu_{ij}(a) = \frac{1}{2\pi} \sqrt{\frac{k_{ij}(a)}{m}}$$



Einstein model

VASP model

Frenkel method



$$F_i(T, a) = E_i^0(a) - k_B T \sum_{j=x,y,z} \ln Z_{ij}$$

$$= E_i^0 - k_B T \sum_{j=x,y,z} \ln \left(\frac{\exp(-h\nu_{ij}/2k_B T)}{1 - \exp(-h\nu_{ij}/k_B T)} \right)$$

$$E_{\text{total}} = \lambda E_{\text{VASP}} + (1 - \lambda) E_{\text{Einstein}}$$

$$\frac{\partial E}{\partial \lambda} = E_{\text{VASP}} - E_{\text{Einstein}}$$

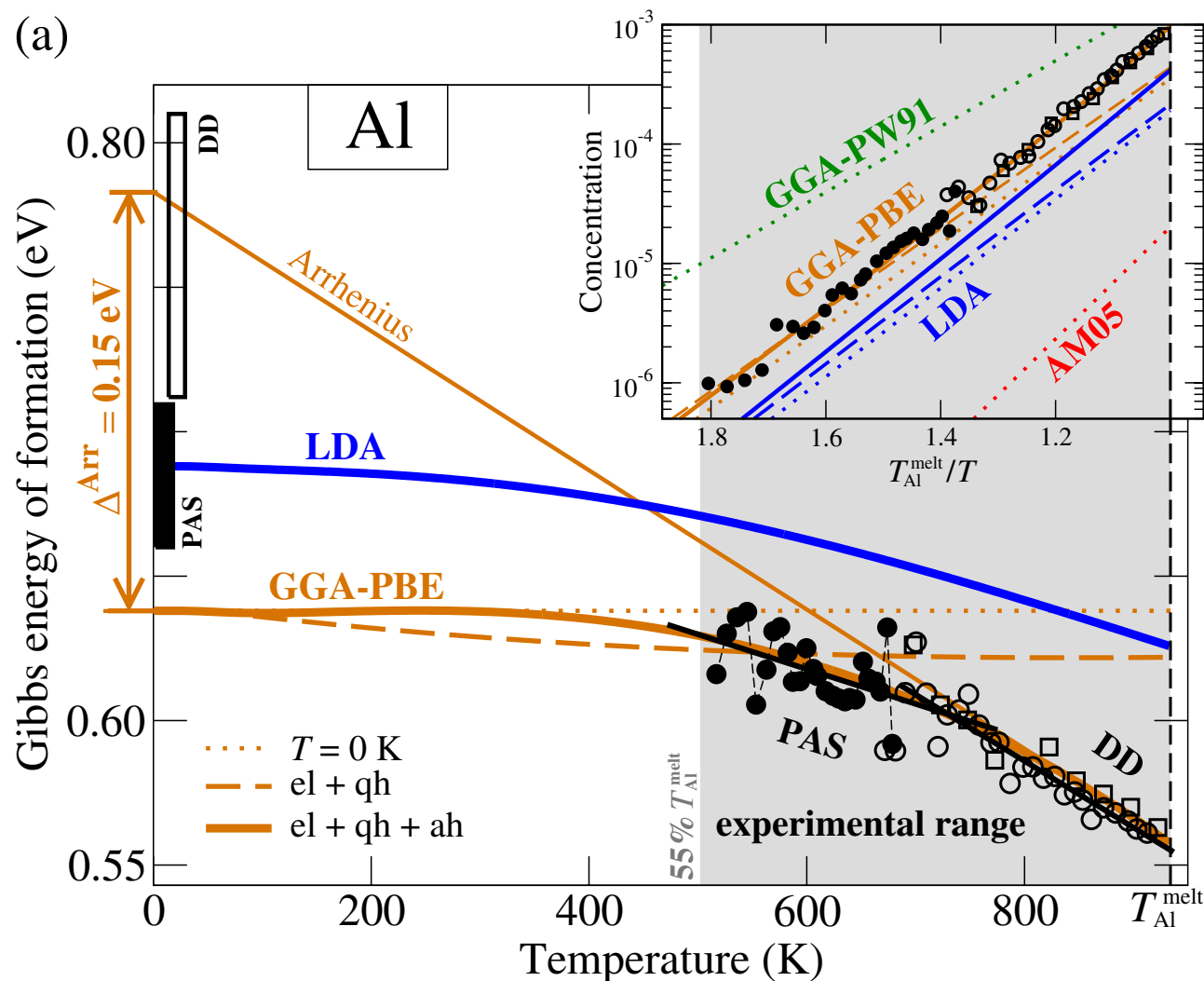
$$F_{\text{VASP}} = F_{\text{Einstein}} + \int_{\lambda=0}^{\lambda=1} \left\langle \frac{\partial E}{\partial \lambda} \right\rangle d\lambda$$

Mono vacancy
(Anharmonicity?)

Breakdown of the Arrhenius Law in Describing Vacancy Formation Energies: The Importance of Local Anharmonicity Revealed by *Ab initio* Thermodynamics

A. Glensk, B. Grabowski, T. Hickel, and J. Neugebauer

UP-TILD(upsampled thermodynamic integration using Langevin dynamics)



Phonon calculations for obtaining the quasiharmonic free energy F^{qh} were done in 2^3 and 3^3 supercells, and nine volume points were found for both elements to ensure converged vibrational free-energy contributions. We also carefully

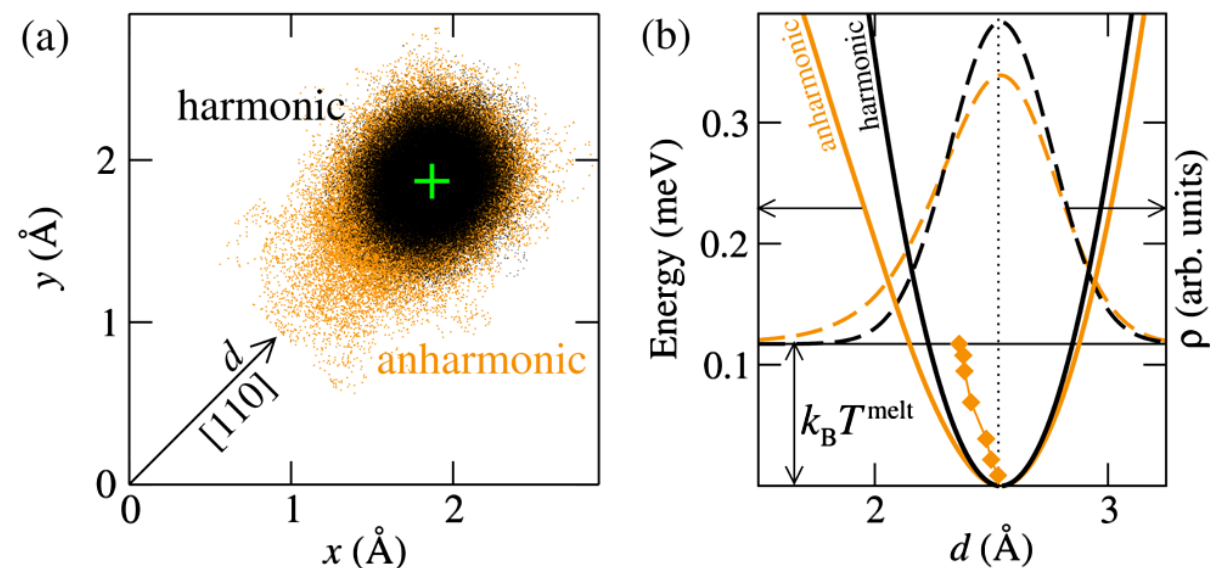
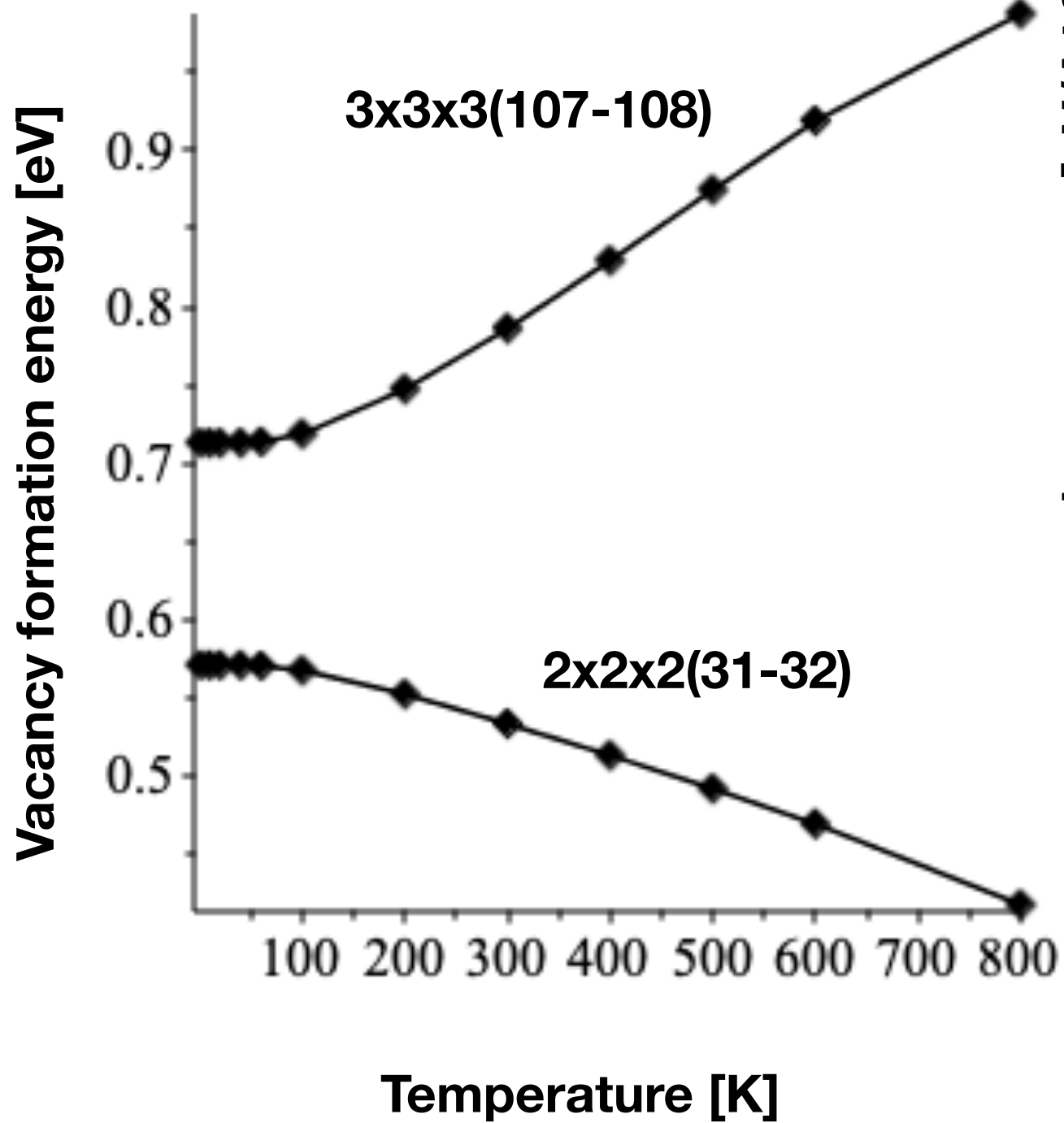


FIG. 3 (color online). (a) Harmonic (black) and anharmonic (orange) distribution $\rho_{V,T}(x,y)$ according to Eq. (5) for Cu at $T^{melt} = 1360 \text{ K}$. The vacancy center is placed at $(0,0)$, and the

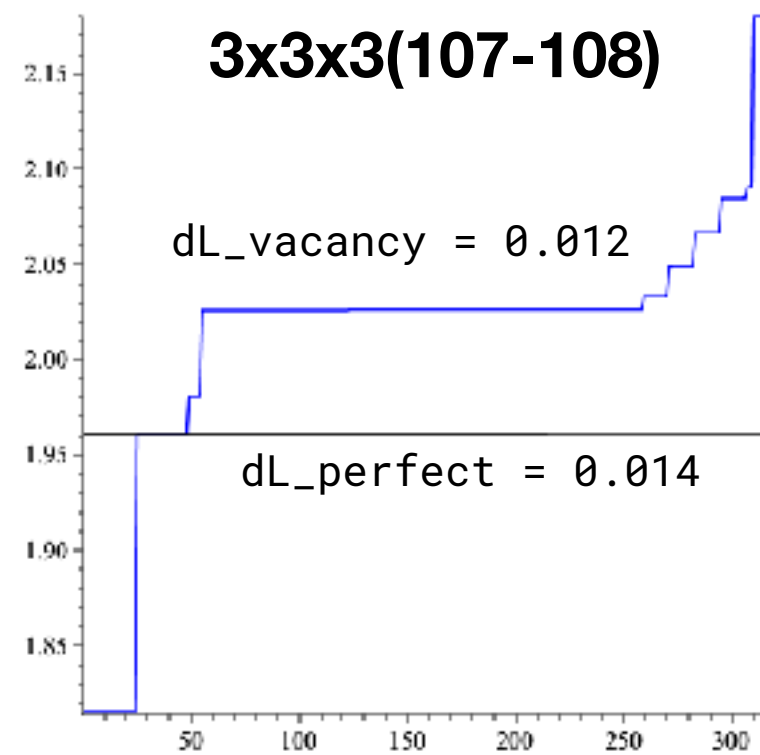
The anharmonic free energy F^{ah} was investigated in a 2^3 (32 atoms) and a 3^3 (108 atoms) supercell and treated with the UP-TILD method [22]. The corresponding molecular-dynamics simulations used a time step of 10 fs and a friction parameter of 0.01 for Al and 0.03 for Cu for the

Vacancy formation energy

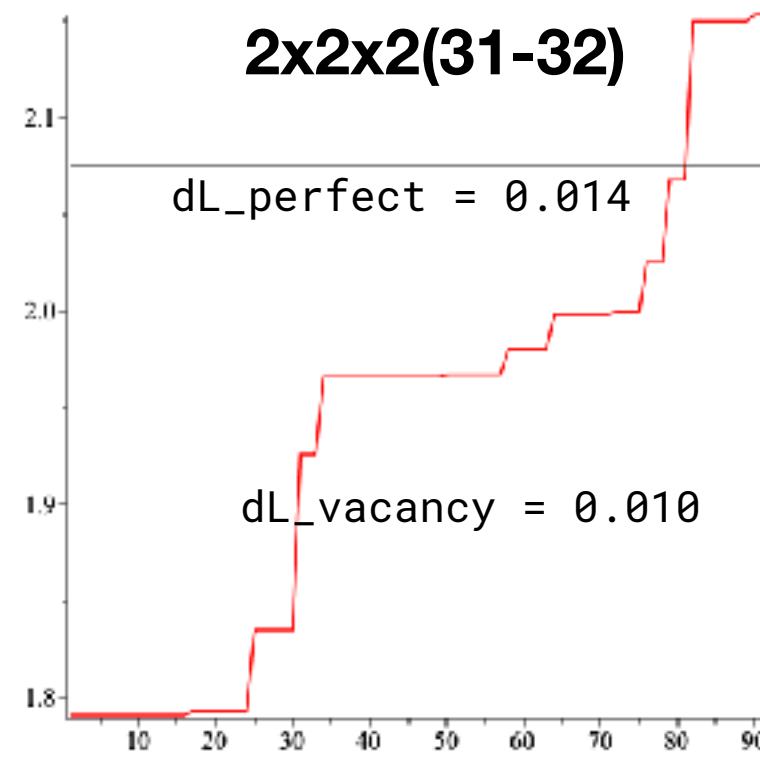


spring constant dispersion (at 500K)

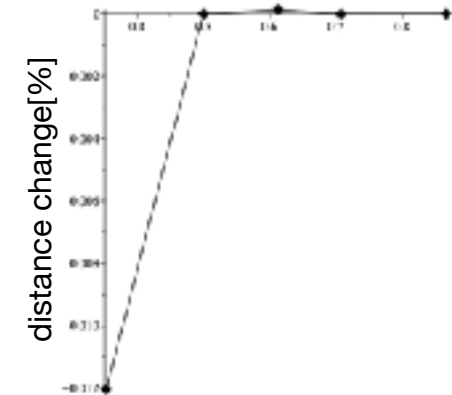
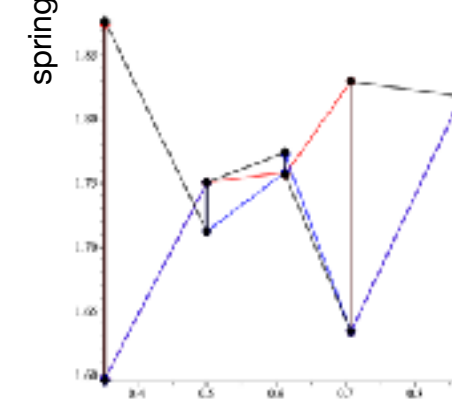
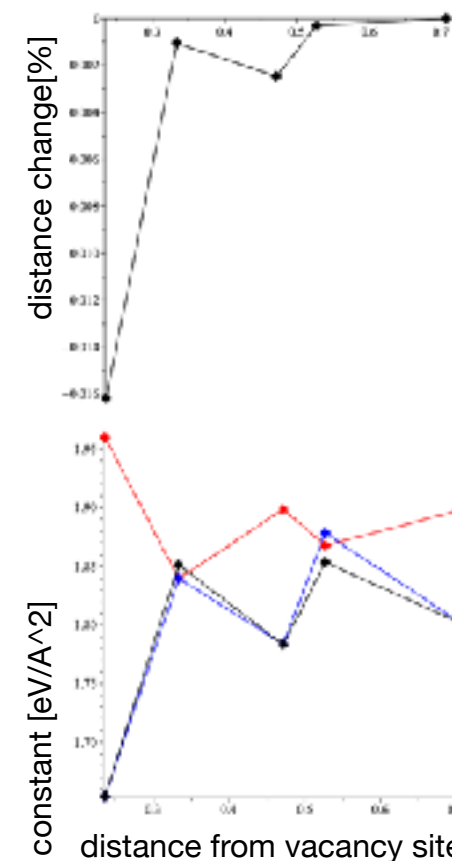
spring constant [eV/A²]



spring constant [eV/A²]



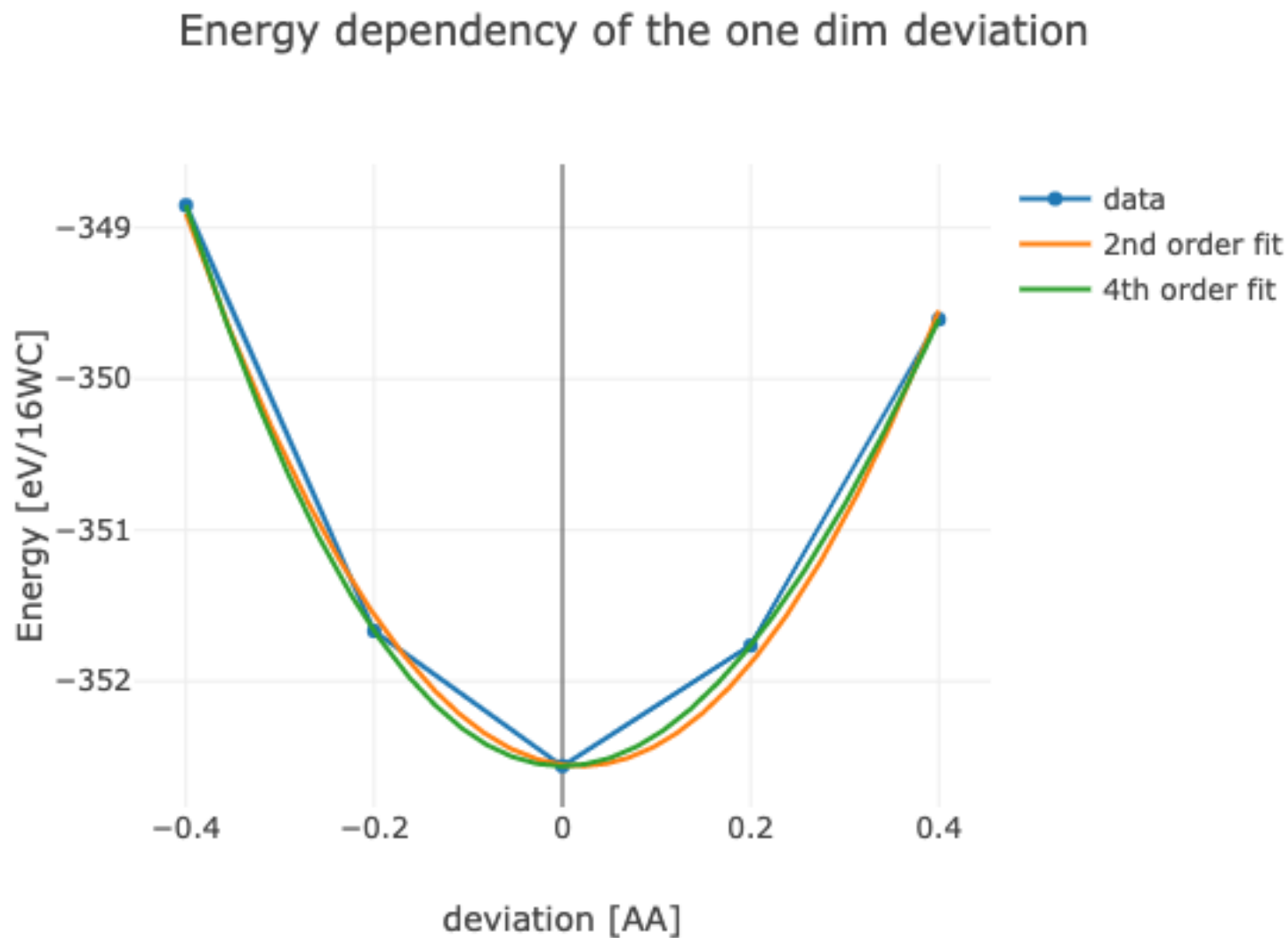
site-direction



Perfect lattice
(Moment +
Frenkel-Ladd(MC))

□ SMM (Statistical Moment Method)

WC



$$E = E_0 + \frac{\partial E}{\partial x_i} dx_i + \frac{\partial^2 E}{\partial x_i^2} dx_i^2 + \frac{\partial^3 E}{\partial x_i^3} dx_i^3 + \frac{\partial^4 E}{\partial x_i^4} dx_i^4$$

0th	-352.5518	-352.5603
1st	-0.8025	-0.0067
2nd	20.7770	21.2321
3rd	0.0	-5.8513
4th	0.0	-2.5690

N. Tan, V. V. Hung, “Investigation of the Thermodynamic Properties of Anharmonic Crystals by the Momentum Method”, Phys. Stat. Sol. (B), vol. 149, pp.511–519, 1988.

$$F_{\text{anharm}} \approx E_0 + F_{\text{harm}} \quad \theta = k_{\text{B}}T, x = \frac{\hbar\omega}{2\theta}$$

$$+3 \left\{ \frac{\theta^2}{k^2} \left[\gamma_2 x^2 \coth^2 x - \frac{2\gamma_1}{3} \left(1 + \frac{x \coth x}{2} \right) \right] \right. \\ \left. + \frac{2\theta^3}{k^4} \left[\frac{4}{3} \gamma_2^2 x \coth x \left(1 + \frac{x \coth x}{2} \right) \right. \right. \\ \left. \left. - 2(\gamma_1^2 + 2\gamma_1\gamma_2) \left(1 + \frac{x \coth x}{2} \right) (1 + x \coth x) \right] \right\},$$

$$E_0 \equiv \sum_j \varphi(|a_j|),$$

$$F_{\text{harm}} = \theta[x + \log(1 - e^{-2x})],$$

$$k = \frac{1}{2} \sum_j \left(\frac{\partial^2 \varphi_{j0}}{\partial u_j^2} \right) = m\omega^2$$

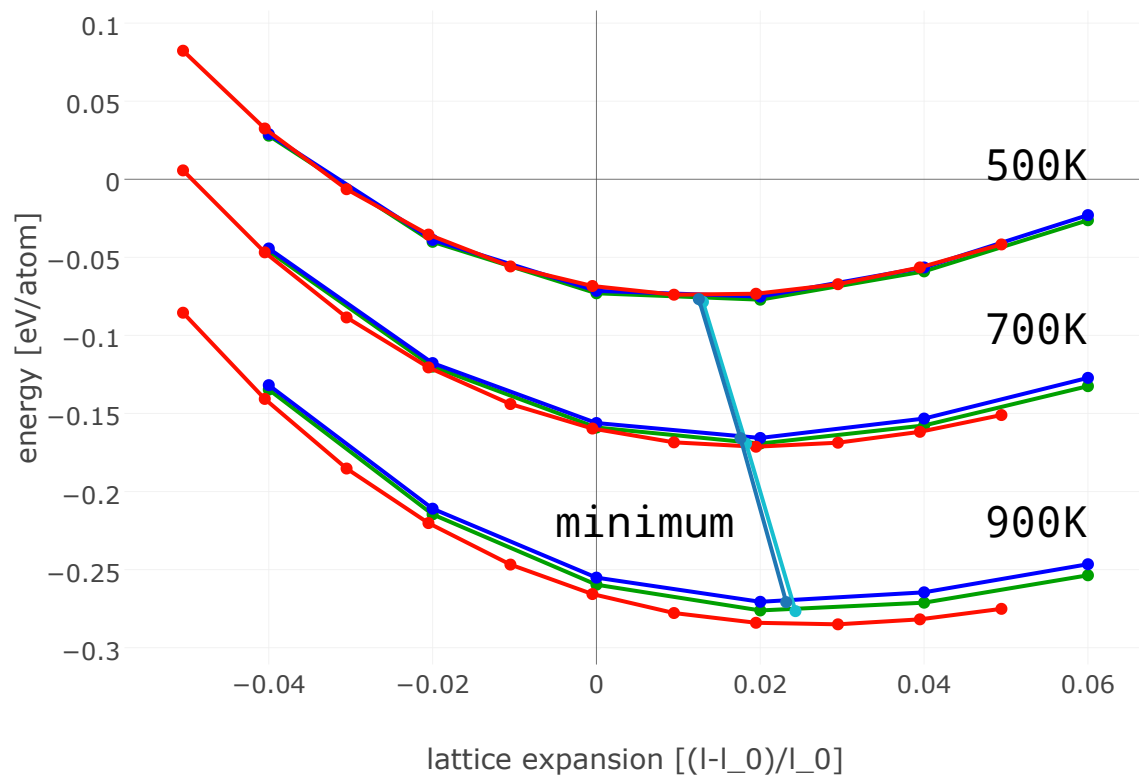
$$\gamma_1 = \frac{1}{48} \sum_j \frac{\partial^4 \varphi_{j0}}{\partial u_{j\beta}^4}, \gamma_2 = \frac{6}{48} \sum_j \frac{\partial^4 \varphi_{j0}}{\partial u_{j\alpha}^2 \partial u_{j\beta}^2}$$

$$E_{\text{higher}}(l') = E_0(l') + \sum_{[k,l,m]} k_{klm}(l') \delta x^k \times \delta y^l \times \delta z^m$$

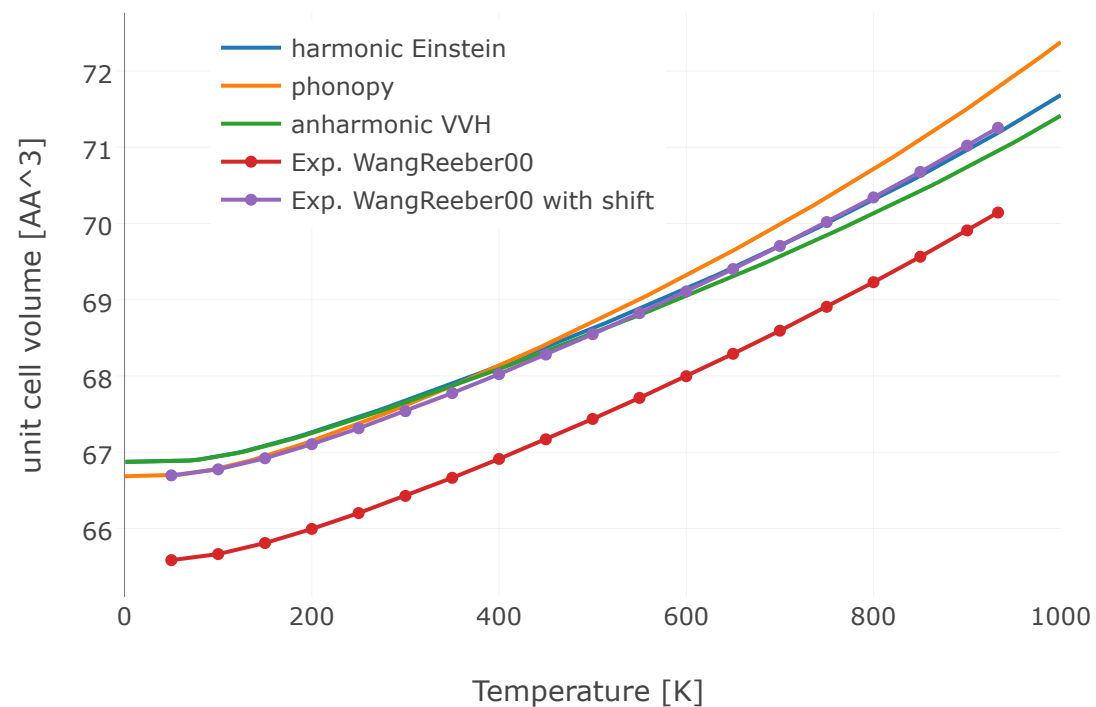
TABLE I. Higher order coefficients of the energy potential.

indexes	analytical	numerical	numerical	harmonic	VASP(2x2x2)	VASP(2x2x2)	VASP(3x3x3)
		p4 dev.=0.04	p4 dev.=0.10		dev.=0.04	dev.=0.10	dev.=0.10
0 [0 0 0]	-2.47840	-2.47840	-2.47840	-3.72303	-3.69879	-3.723027	
1 [2 0 0]	6.60522	6.60496	6.60288	6.66320	3.30538	3.37042	4.26487
2 [0 2 0]	6.60522	6.60496	6.60288	6.66320	3.33010	3.35011	4.27330
3 [0 0 2]	6.60522	6.60496	6.60288	6.66320	3.39418	3.35422	4.28811
4 [0 1 1]		1.720e-12	2.842e-13		0.02135	0.01158	-0.00212
5 [1 1 0]		1.600e-11	-1.125e-12		-0.02505	-0.01058	0.00217
6 [1 0 1]		1.720e-12	8.527e-13		0.03010	0.01165	-0.00154
7 [3 0 0]		-2.852e-09	-1.218e-10		-0.05000	0.00020	0.00054
8 [0 3 0]		-1.158e-09	-5.801e-11		-0.25417	-0.00222	0.00374
9 [0 0 3]		-2.147e-09	2.404e-11		0.25833	-0.00588	0.02284
10 [1 1 1]		-2.224e-26	-8.807e-12		-0.04375	0.00024	0.00056
11 [2 2 0]	29.14519	29.23755	29.34441		53.12500	9.96245	10.62694
12 [2 0 2]	29.14519	29.23755	29.34441		46.30102	9.91347	10.73143
13 [0 2 2]	29.14519	29.23755	29.34441		40.24235	10.46694	10.46041
14 [4 0 0]	6.35142	6.51689	6.84933		-3.54167	0.30400	-0.56800
15 [0 4 0]	6.35142	6.51690	6.84933		-14.47916	2.01067	-1.22133
16 [0 0 4]	6.35142	6.51689	6.84933		-47.29167	1.58400	-2.62133
standard dev.		0.000000	0.000014		0.000025	0.000047	0.000031

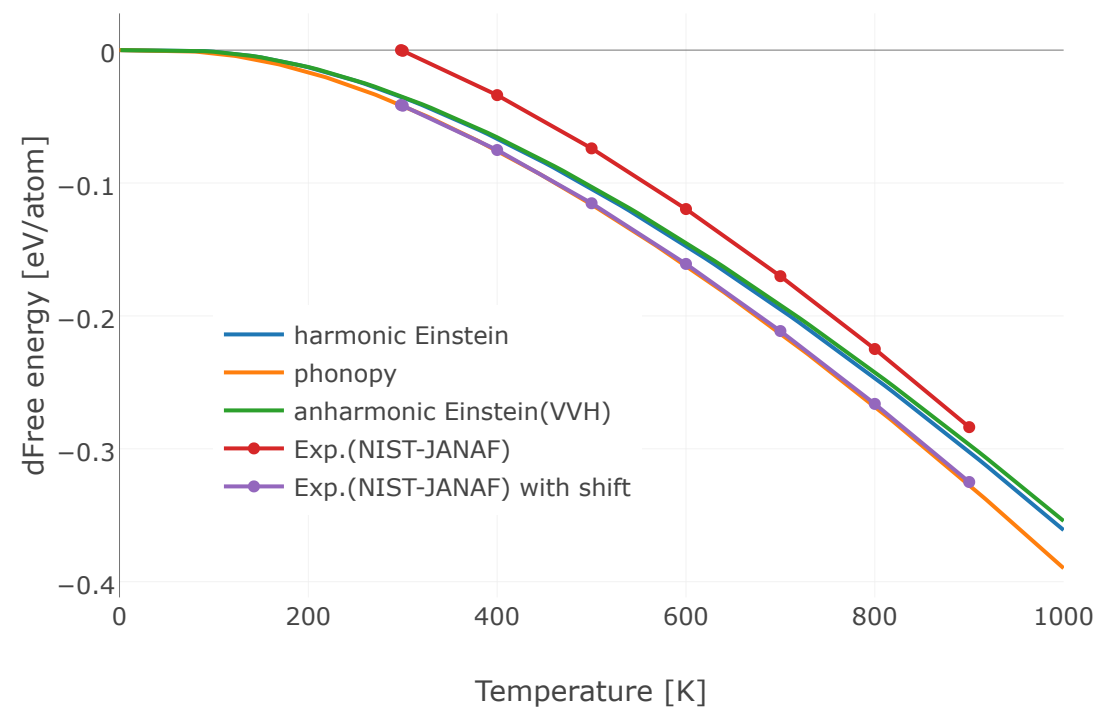
Free energy- volume curves



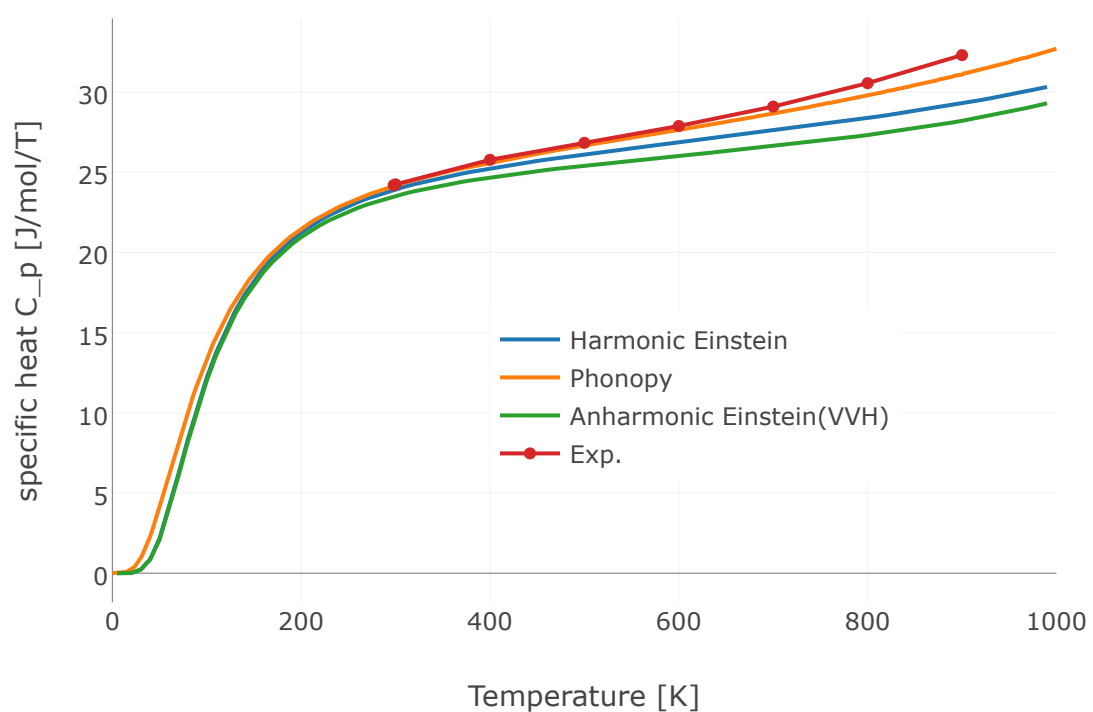
Volume



Free energy



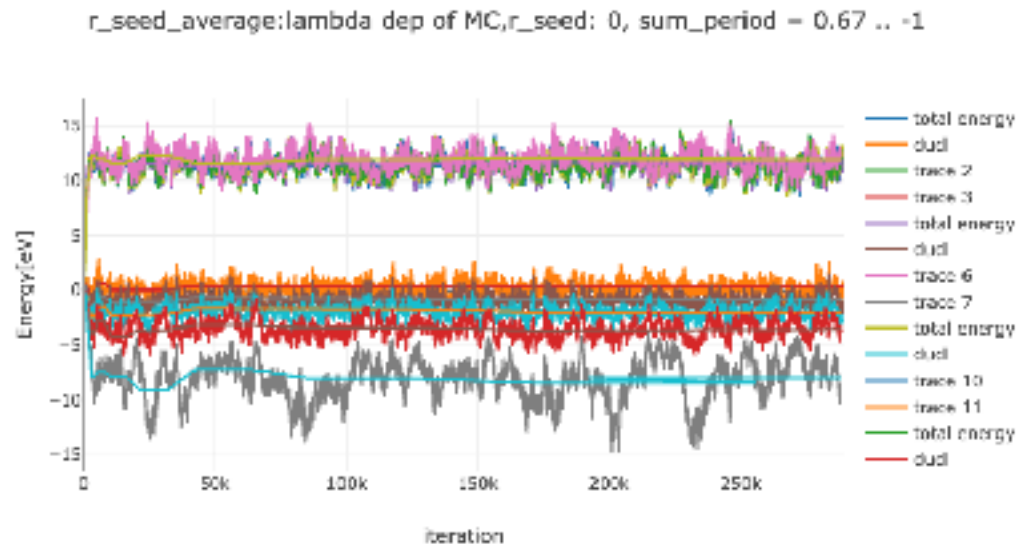
specific heat C_p



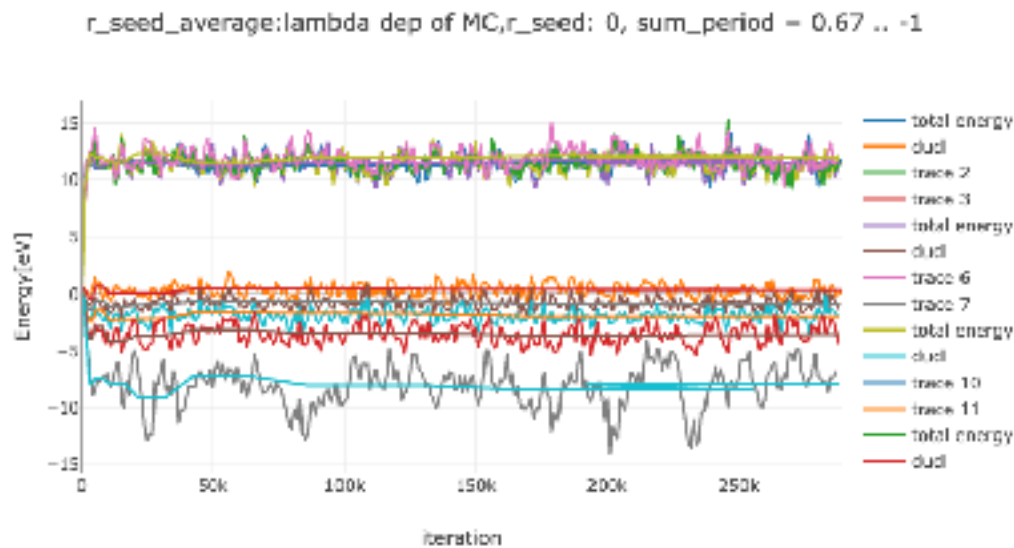
LJ-Frenkel

./frenkel/p3_lj/figs

skip=1

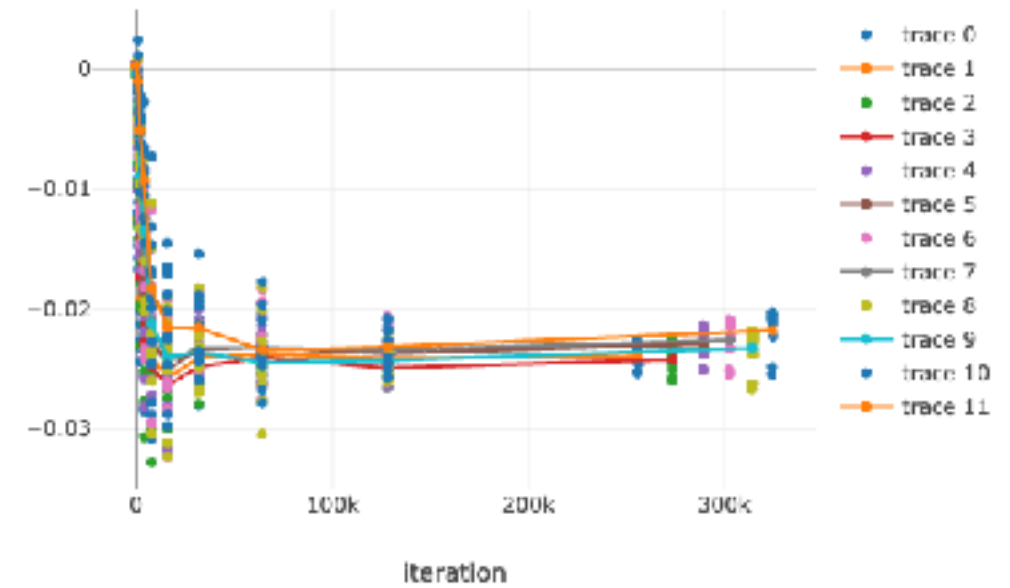


skip=1000



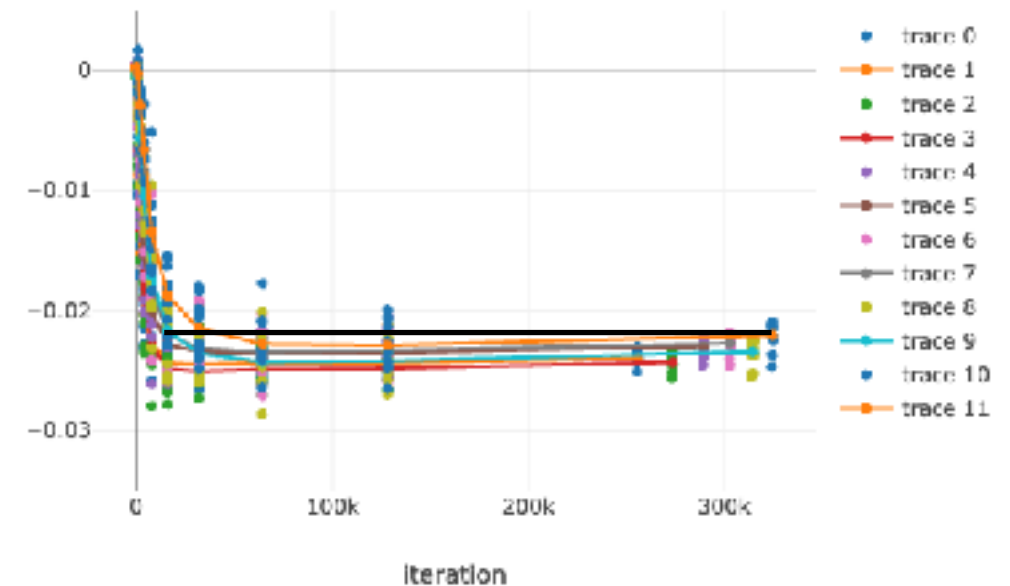
sum 067

Monte Carlo simulation

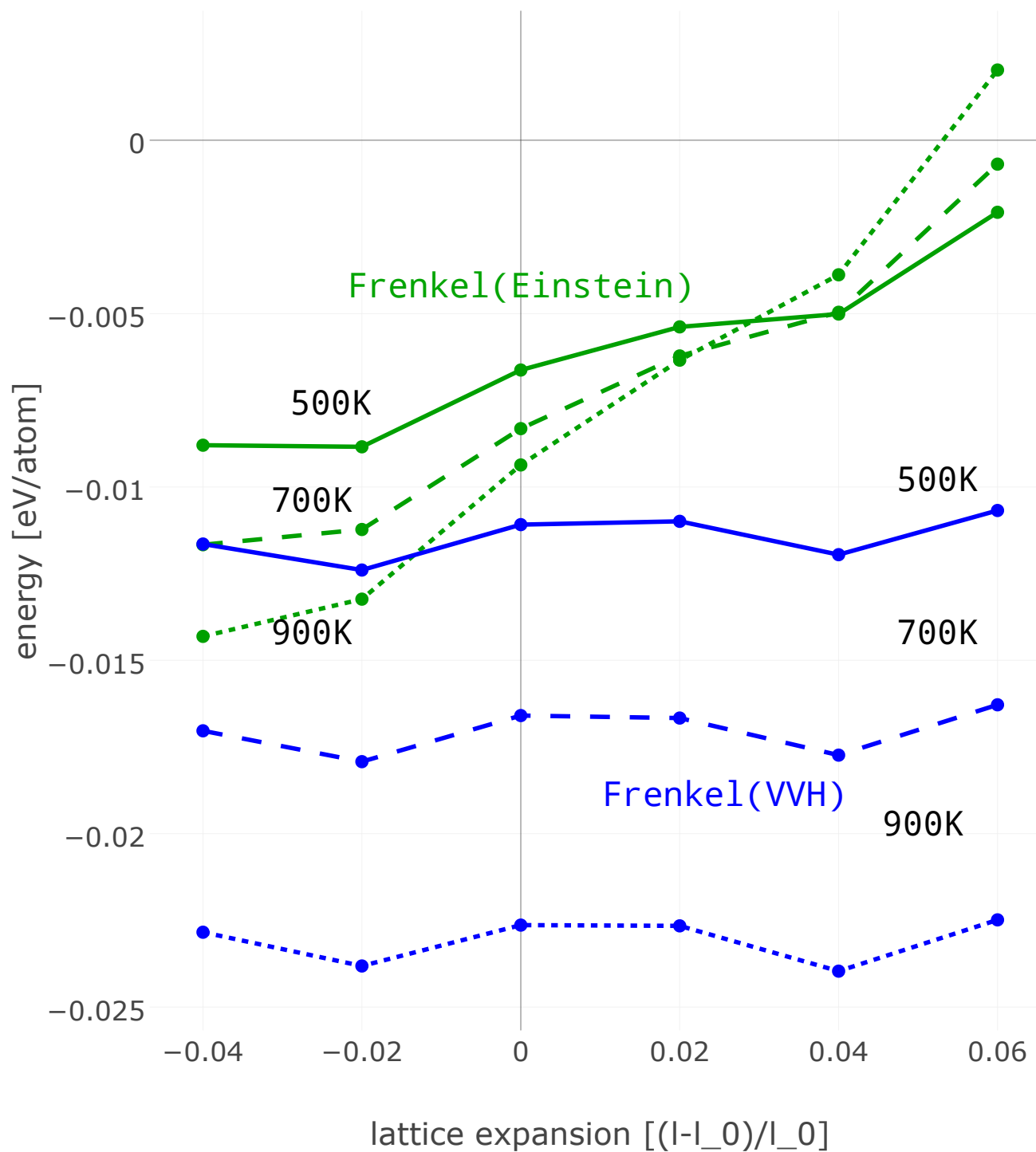


sum 020

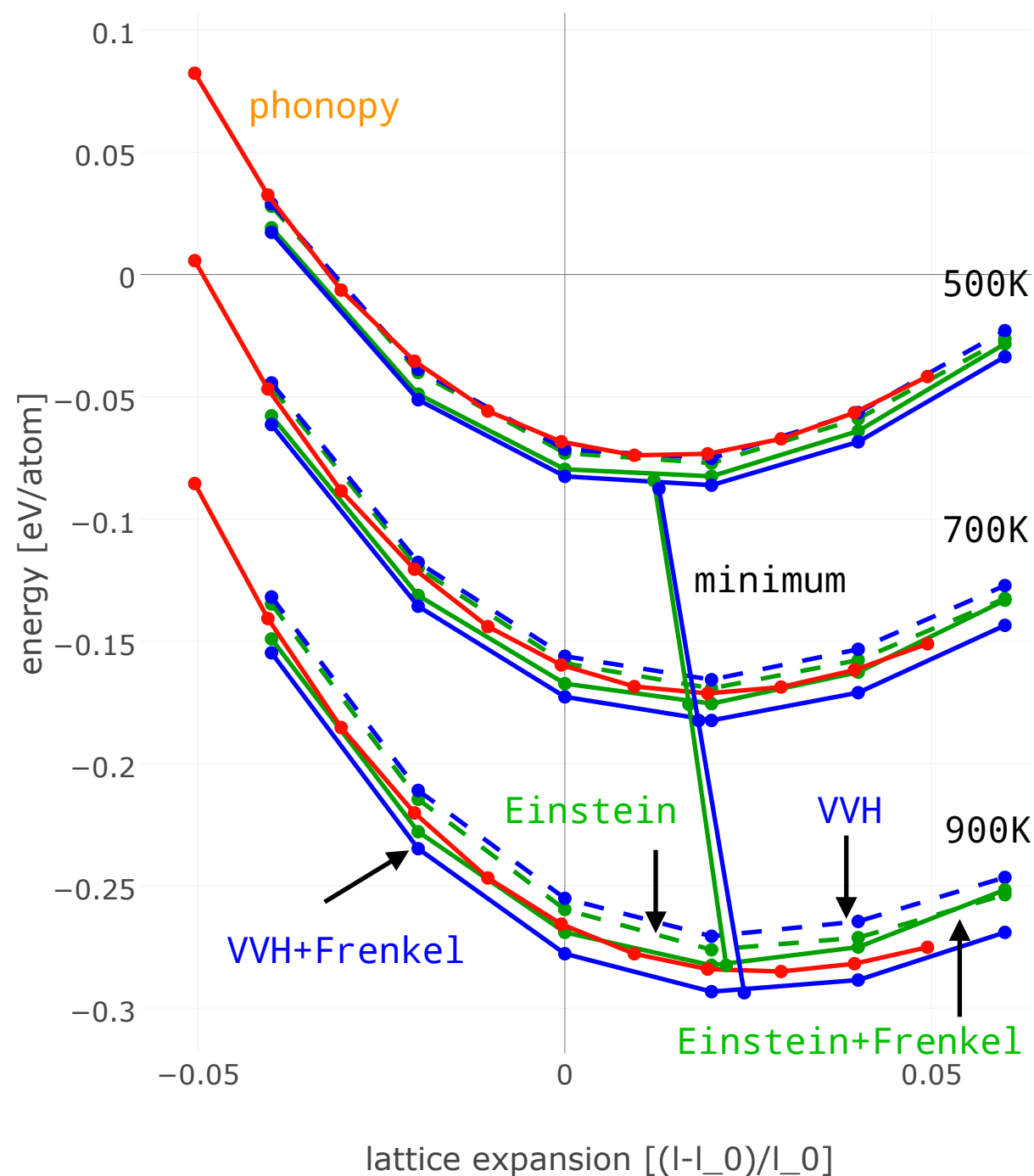
Monte Carlo simulation



Frenkel integrated anharmonic free energy



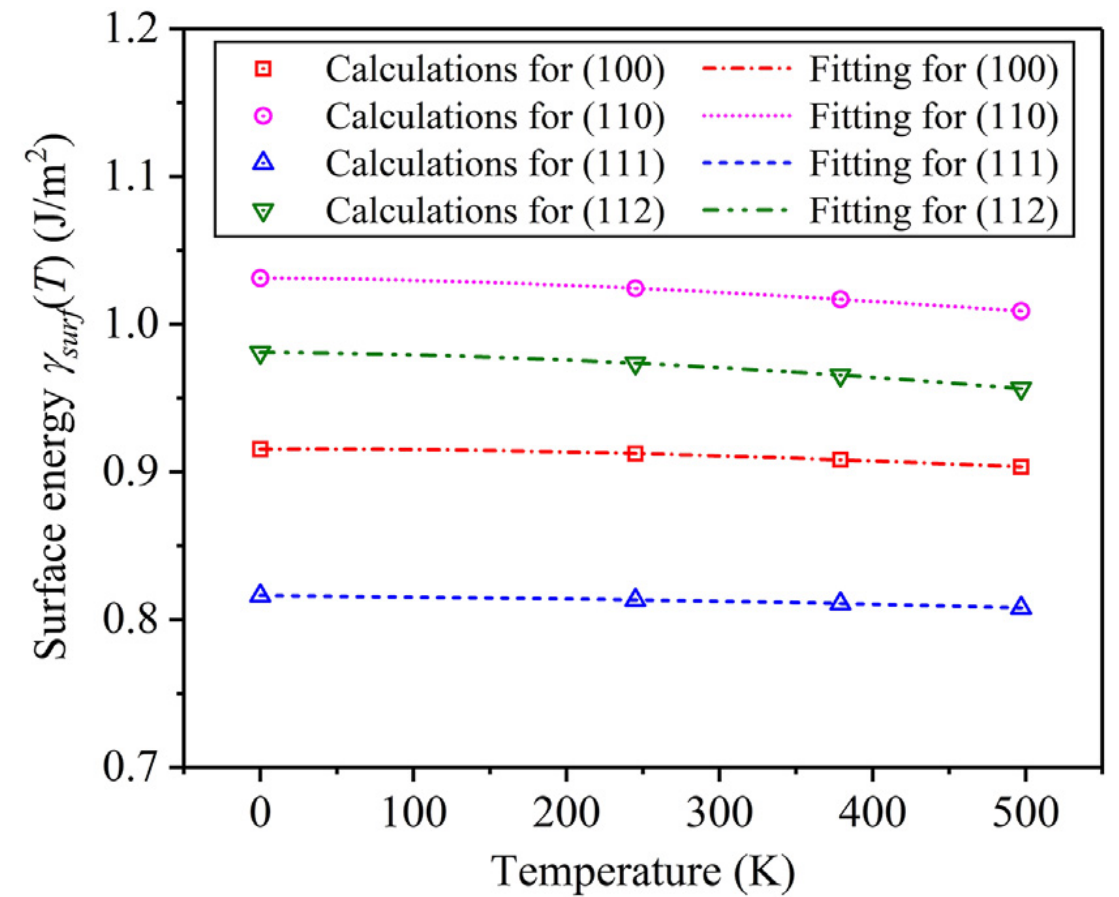
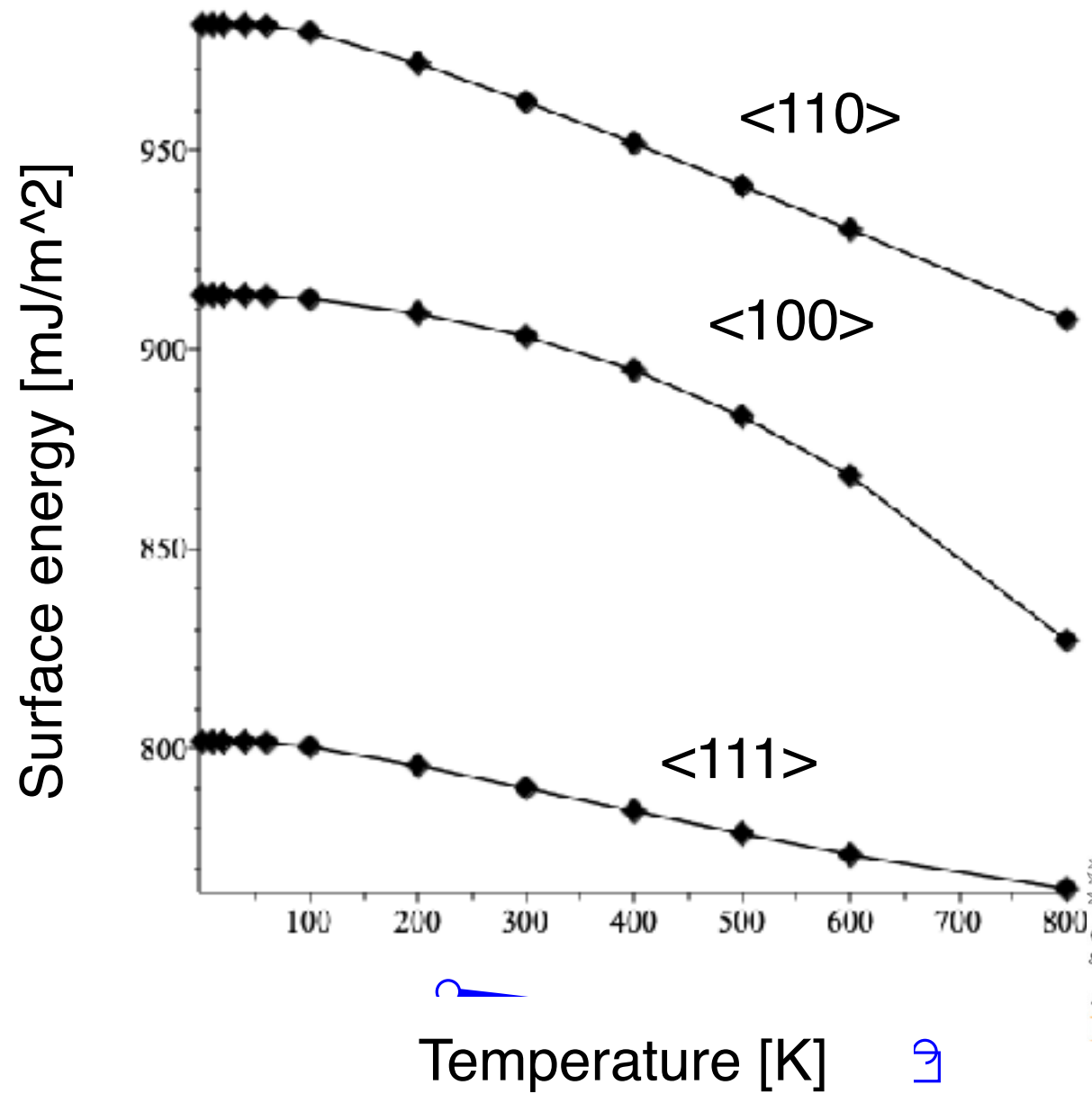
Free energy- volume curves



Surface
(MC simulations)

Einstein model of Al

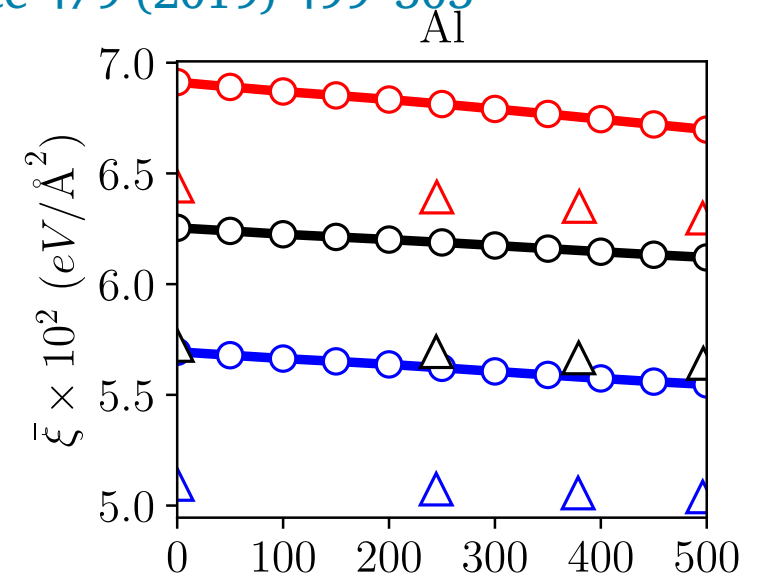
surface



Effects of finite temperature on the surface energy in Al alloys from first-principles calculations

Zhipeng Wang^{a,1}, Dongchu Chen^{b,1}, Qihong Fang^{a,*}, Hong Chen^{b,*}, Touwen Fan^{b,*}, Bin Liu^c, Feng Liu^c, Pingying Tang^d

Applied Surface Science 479 (2019) 499–505

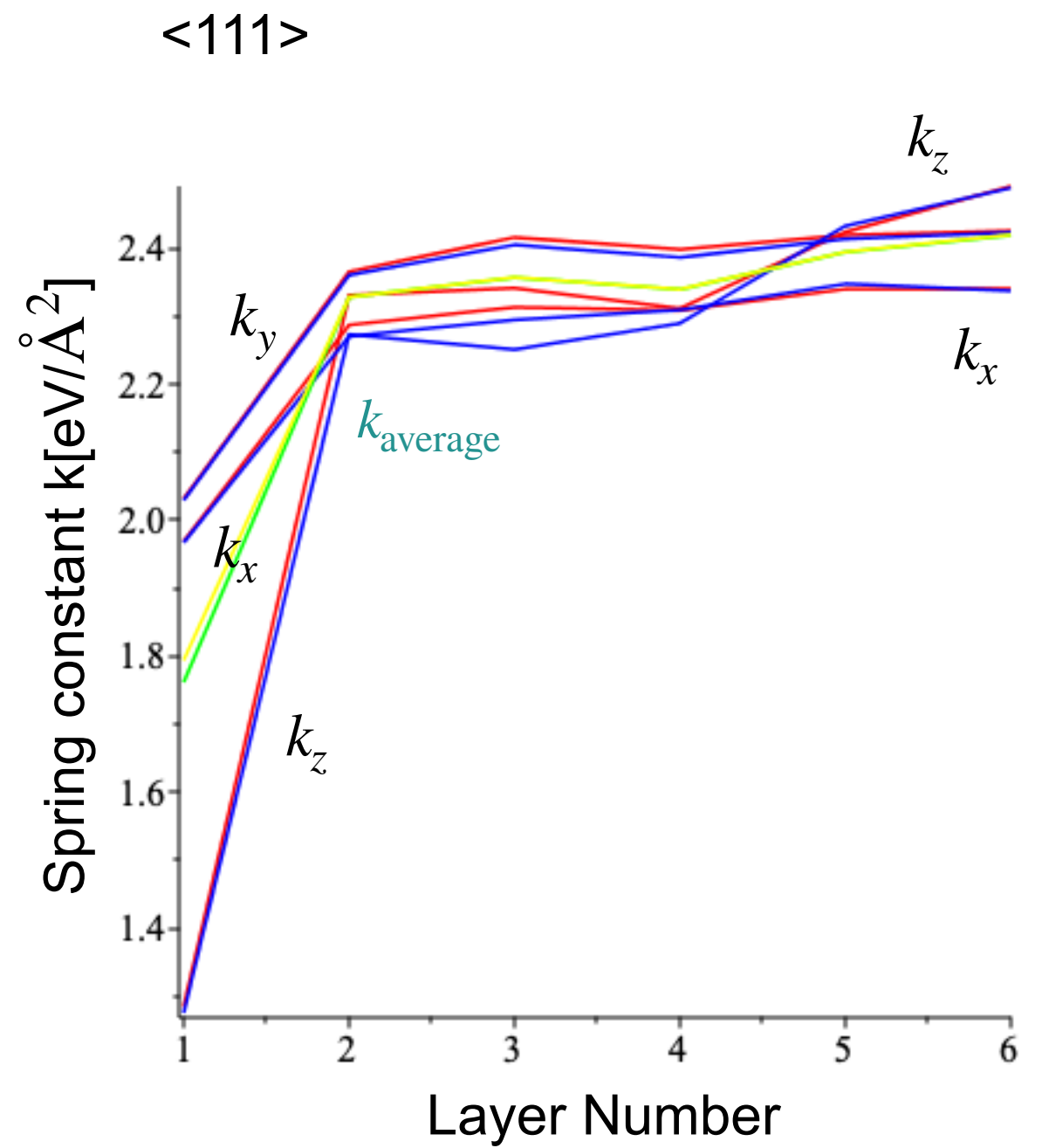
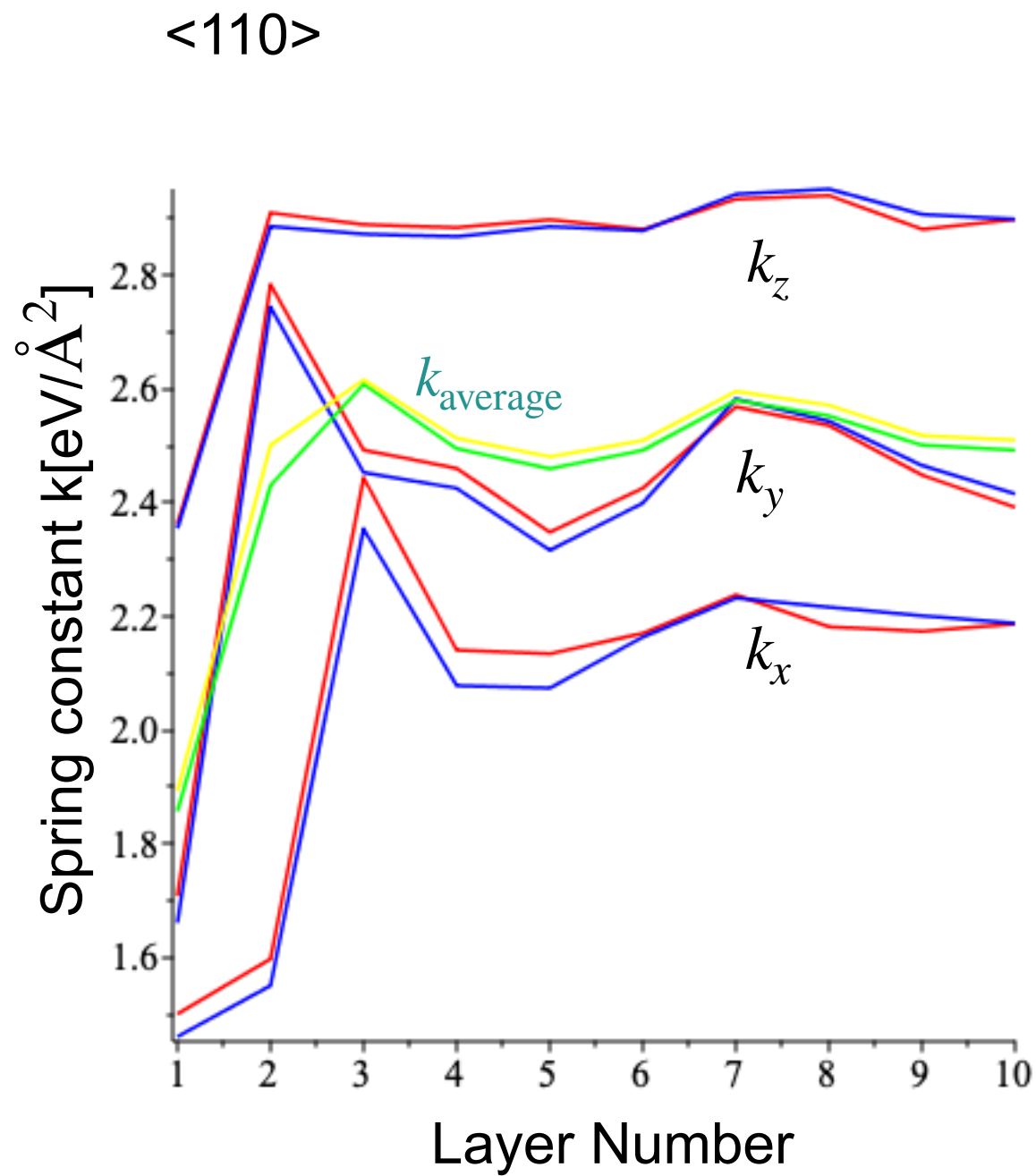


A fast atomistic approach to finite-temperature surface elasticity of crystalline solids

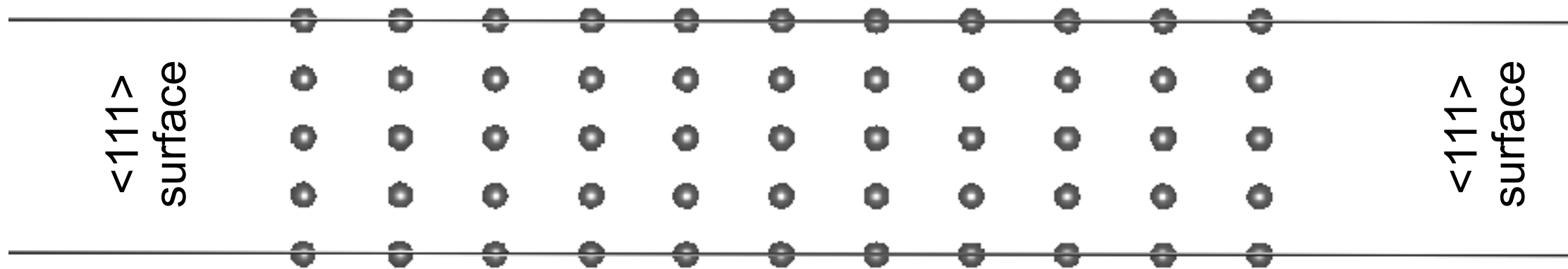
Shashank Saxena^a, Miguel Spinola^a, Prateek Gupta^b, Dennis M. Kochmann^{a,*}

Computational Materials Science 211 (2022) 111511

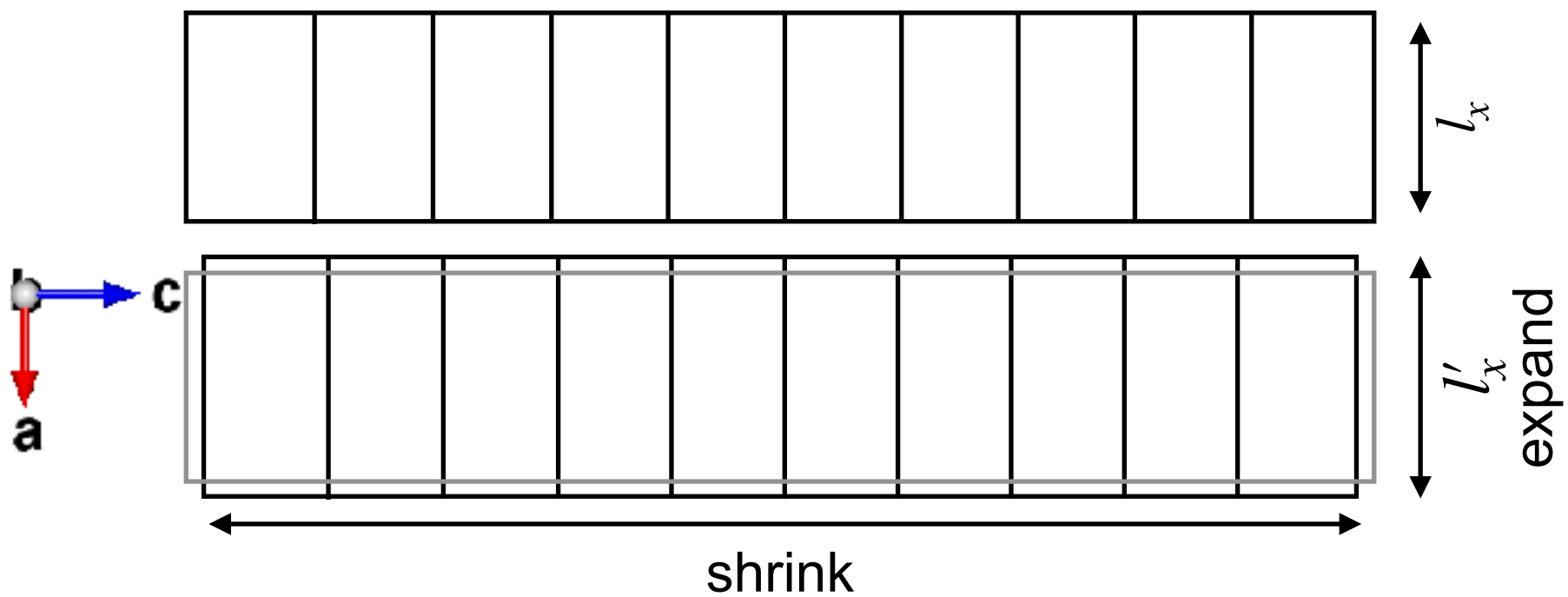
Layer dependency of spring constants

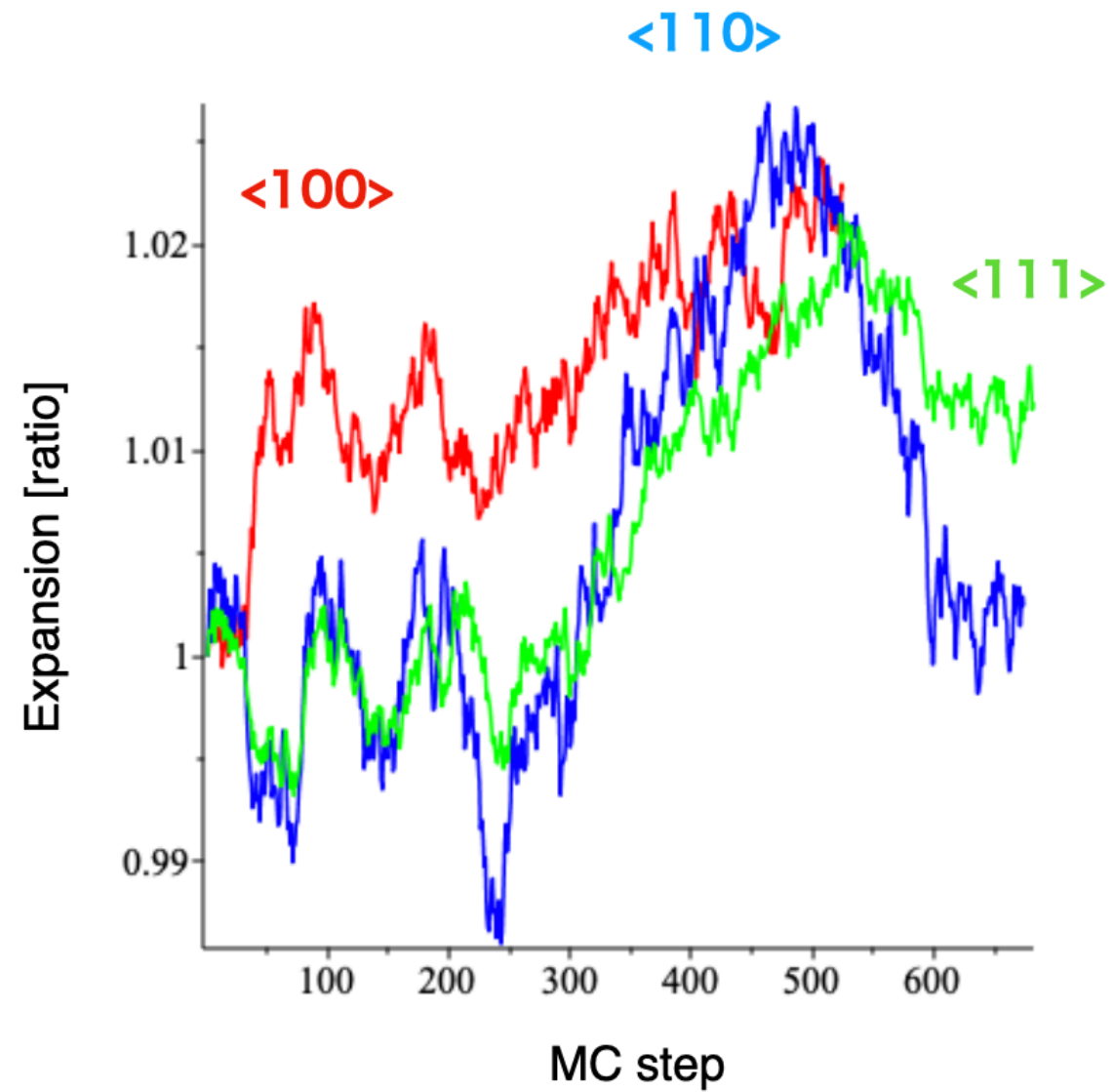


Slab model



0
Distance z [\AA]





Surface expansion during MC simulation.

修士論文

Al表面の有限温度第一原理計算

summary

1. Lattice defects free energy
 1. Vacancy, Surface
2. Einstein(Harmonic) + Frenkel-Ladd(Anharmonic)
3. Boundary (Harm. + small Anharm.)
4. Vacancy (Harm.: ?)
5. Perfect (Moment method)
 1. Volume, but ...
6. Surface
 1. Harm.:X, Anharm.:?